Liquid-vapor interfaces in *XY*-spin fluids: An inhomogeneous anisotropic integral-equation approach

I. P. Omelyan,[1,2] R. Folk,[2] A. Kovalenko,[3] W. Fenz,[2] and I. M. Mryglod[1,2]
[1]*Institute for Condensed Matter Physics, National Academy of Sciences of Ukraine, 1 Svientsitskii Street, UA-79011 Lviv, Ukraine*
[2]*Institute for Theoretical Physics, Linz University, A-4040 Linz, Austria*
[3]*National Institute for Nanotechnology, National Research Council, and Department of Mechanical Engineering, University of Alberta, 11421 Saskatchewan Drive, Edmonton, AB, Canada T6G 2M9*
(Received 26 September 2008; published 22 January 2009)

An integral-equation approach is developed to study interfacial properties of anisotropic fluids with planar spins in the presence of an external magnetic field. The approach is based on the coupled set of the Lovett-Mou-Buff-Wertheim integro-differential equation for the inhomogeneous anisotropic one-particle density and the Ornstein-Zernike equation for the orientationally dependent two-particle correlation functions. Using the proposed inhomogeneous angle-harmonics expansion formalism we show that these integral equations can be reduced to a much simpler form similar to that inherent for a system of isotropic fluids. The interfacial orientationally dependent direct correlation function can be consistently constructed by means of a nonlinear interpolation via its values obtained in the coexisting anisotropic bulk phases. A soft mean spherical approximation is employed for the closure relation. This has allowed us to solve the complicated integral equations in the situation when both spatial inhomogeneity and orientational anisotropy are present simultaneously. The approach introduced is applied to an *XY* fluid model with ferromagnetic spin interactions. As a result, the density-orientation and magnetization profiles at the liquid-vapor interfaces are calculated in a wide range of temperatures up to subcritical regions. The influence of the external field on the microscopic structure of the interfaces and the surface tension is also analyzed in detail.

DOI: 10.1103/PhysRevE.79.011123 PACS number(s): 64.60.−i, 64.70.F−, 68.03.−g, 75.50.Mm

I. INTRODUCTION

An unsettled problem in studies of inhomogeneous properties of fluids is the determination of the microscopic structure at liquid-vapor interfaces [1,2]. These interfaces appear in many physical, chemical, and biological systems. A lot of phenomena such as condensation and evaporation, wetting, and drying, etc., can be observed in an interfacial liquid-vapor surrounding. The investigation of interfaces is important for fundamental theoretical purposes as well as for various technological applications.

Inhomogeneities in fluids have attracted considerable attention over the last decades. The microscopic theoretical modeling of liquid-vapor and liquid-liquid interfaces has been performed by the integral-equation method [1,3–10], the density-functional formalism [11–18], capillary-wave theories [19–22], as well as computer simulation techniques [18,23–32]. Most of these works were focused mainly on the consideration of simple isotropic fluid models, such as Lennard-Jones (LJ) or LJ-like systems and their mixtures. The theoretical approaches were based on the Born-Green-Yvon (BGY) [3] or Lovett-Mou-Buff-Wertheim (LMBW) [5,6] integro-differential equations for inhomogeneous one-particle density functions. The two-particle correlation functions are usually interpolated within the inhomogeneous region using their bulk values in the coexisting phases [7,8]. The bulk functions are found from the homogeneous Ornstein-Zernike (OZ) equations complemented by a certain closure relation. For simple LJ fluids, the one- and two-particle correlation functions can be calculated by solving the coupled set of the inhomogeneous OZ (IOZ) and LMBW equations [9,10].

Interfacial properties of systems with anisotropic interactions between particles were considered as well. In particular, for a model of homonuclear diatomic molecules, the structure and surface tension of the liquid-vapor interface have been evaluated employing perturbation and integral-equation theories [33,34]. An integral-equation formulation for dipolar fluids has been developed in Refs. [35,36]. As a result, the orientation profiles at liquid-vapor and polar-nonpolar liquid interfaces were calculated for the Stockmayer model of water. Theoretical predictions on molecular alignment at the liquid-vapor interface of dipolar fluids were examined versus simulation and experimental results [37]. Orientational transitions of anisotropic nanoparticles at liquid-liquid interfaces were investigated in Ref. [38]. An extension of the integral equations to polyatomic fluids with Coulomb site-site interactions has been carried out in Ref. [39].

Quite recently, a generalization of the LMBW-OZ integral-equation concept to magnetic fluids has also been performed [40]. However, this generalization concerns the simplest Ising spin model which is reduced to a binary nonmagnetic mixture. Until now, there were no attempts to consider interfacial properties of a more complicated *XY*-spin model of magnetic fluids when both spatial inhomogeneity and orientational anisotropy exist in the system simultaneously. Note that the *XY* system may play an important role in describing superfluid and demixing transitions in ^{2}He-^{4}He mixtures [41–43]. It is worth emphasizing that the existing anisotropic inhomogeneous integral-equation theories [33–37] are valid only for dipolar or polar systems and are not applicable to *XY* fluids. The reason is that the specific ferromagnetic spin interactions cannot be expressed in

spherical harmonics as it can be done for dipole potentials.

It has been shown within a homogeneous integral-equation description that bulk phase properties of *XY*-spin fluids can readily be obtained by expanding one- and two-body correlation functions in terms of planar harmonics [44–46]. Note that the *XY* fluids exhibit a rich variety of phase diagrams which are similar to those of Ising and Heisenberg spin models [47–50]. Like for simple nonmagnetic fluids, they are characterized by the existence of a liquid-vapor phase transition. This transition is due to attractive interactions which arise between particles with parallel spin orientations. Moreover, in the absence of an external magnetic field, the transitions between paramagnetic and ferromagnetic states appear additionally. Such a complexity can be explained by a coupling between the translational and spin degrees of freedom.

In this paper we develop an inhomogeneous integral-equation approach for anisotropic magnetic fluids with planar spin interactions. The main idea consists in the extension of the angle-harmonics expansion formalism to the interfacial correlation functions. Then the cumbersome set of integro-differential equations can be simplified significantly and cast in an isotropiclike form. As a consequence, the liquid-vapor interfacial properties of the *XY* fluid model have been calculated for the first time.

The rest of the paper is organized as follows. In Sec. II we will describe the model under study and the proposed integral-equation theory. The obtained results will be presented and discussed in Sec. III. The main conclusions of this work are outlined in Sec. IV.

II. THEORY

A. *XY*-spin fluid model

Consider a classical *XY*-spin fluid model described by the Hamiltonian

$$H=\sum_{i<j}^{N}[\phi(r_{ij})-J(r_{ij})\mathbf{s}_i\cdot\mathbf{s}_j]-\sum_{i=1}^{N}\mathbf{B}(\mathbf{r}_i)\cdot\mathbf{s}_i, \tag{1}$$

where $\phi(r_{ij})$ and $J(r_{ij})$ are the potential and exchange integral of nonmagnetic and spin-spin interactions, respectively, depending on the interparticle separation $r_{ij}=|\mathbf{r}_i-\mathbf{r}_j|$ with $\mathbf{r}_i$ being the three-dimensional spatial coordinate of the ith particle carrying planar spin $\mathbf{s}_i$ (of unit length, $|\mathbf{s}_i|=1$) which lies in the *XY* plane, N is the total number of particles, and $\mathbf{B}(\mathbf{r}_i)$ is the external inhomogeneous magnetic field. The exchange integral of ferromagnetic ($J>0$) interactions can be modeled by the Yukawa function

$$J(r)=\frac{\varepsilon\sigma}{r}\exp\left(-\frac{r-\sigma}{\sigma}\right), \tag{2}$$

while the nonmagnetic repulsion can be cast in the form of the LJ-like potential

$$\phi(r)=\begin{cases}4\varepsilon\left[\left(\dfrac{\sigma}{r}\right)^{12}-\left(\dfrac{\sigma}{r}\right)^{6}\right]+\varepsilon, & r<\sqrt[6]{2}\sigma,\\ 0, & r\geqslant\sqrt[6]{2}\sigma,\end{cases} \tag{3}$$

where ε scales the intensity of the interactions and σ denotes the size of the particles.

B. IAOZ-LMBW-SMSA formulation

The Ornstein-Zernike equation generalized to spatially inhomogeneous and orientationally anisotropic spin systems has the form

$$\begin{aligned}h(\mathbf{r}_1,\mathbf{r}_2,\varphi_1,\varphi_2)&=c(\mathbf{r}_1,\mathbf{r}_2,\varphi_1,\varphi_2)\\&+\frac{1}{2\pi}\int_V d\mathbf{r}_3\int_0^{2\pi}d\varphi_3 c(\mathbf{r}_1,\mathbf{r}_3,\varphi_1,\varphi_3)\rho(\mathbf{r}_3,\varphi_3)\\&\times h(\mathbf{r}_3,\mathbf{r}_2,\varphi_3,\varphi_2),\end{aligned} \tag{4}$$

where $h(\mathbf{r}_1,\mathbf{r}_2,\varphi_1,\varphi_2)$ and $c(\mathbf{r}_1,\mathbf{r}_2,\varphi_1,\varphi_2)$ are the two-body total and direct correlation functions, respectively, $\rho(\mathbf{r},\varphi)$ denotes the orientationally dependent one-body number density distribution function, and V the volume of the system. For planar interfaces the inhomogeneous anisotropic Ornstein-Zernike (IAOZ) equation [Eq. (4)] simplifies to

$$\begin{aligned}h(q,z_1,z_2,\varphi_1,\varphi_2)&=c(q,z_1,z_2,\varphi_1,\varphi_2)\\&+\frac{1}{2\pi}\int_Q d\mathbf{q}'\int_{-\infty}^{\infty}dz_3\int_0^{2\pi}d\varphi_3\\&\times c(|\mathbf{q}-\mathbf{q}'|,z_1,z_3,\varphi_1,\varphi_3)\\&\times\rho(z_3,\varphi_3)h(q',z_3,z_2,\varphi_3,\varphi_2).\end{aligned} \tag{5}$$

Here $\mathbf{q}$ is the projection of vector $\mathbf{r}$ on the interfacial xy plane with the surface Q, and z designates the distance to the interface. In such a geometry, the separation between two particles can be presented as $r_{12}=[q_{12}^2+(z_1-z_2)^2]^{1/2}$, where $q_{12}=|\mathbf{q}_1-\mathbf{q}_2|\equiv q$. In the case of the external magnetic field with a fixed direction of its vector $\mathbf{B}$, the angles φ can be referred to the projection $\mathbf{B}_{XY}=\mathbf{B}-(\mathbf{B}\cdot\mathbf{n})\mathbf{n}$ of $\mathbf{B}$ on the spin-*XY* plane. The normal vector $\mathbf{n}$ defines the orientation of the *XY* plane in the laboratory xyz system of coordinates, i.e., its orientation with respect to the interfacial xy plane. Then taking into account that the spin vector $\mathbf{s}$ lies in the *XY* plane, one obtains $\mathbf{B}\cdot\mathbf{s}=\mathbf{B}_{XY}\cdot\mathbf{s}=B_{XY}\cos\varphi$ and $\mathbf{s}_1\cdot\mathbf{s}_2=\cos(\varphi_1-\varphi_2)$. Note that for fixed directions of $\mathbf{B}$ and $\mathbf{n}$, the direction of vector $\mathbf{B}_{XY}$ also remains unchanged. The magnitude $B_{XY}(x,y,z)$ of $\mathbf{B}_{XY}$ can in general vary with x, y, and z. To simplify notations, we will omit the signatures *XY* and (x,y) at $B_{XY}(x,y,z)$ by merely writing $B(z)$.

The one-body density distribution function $\rho(z,\varphi)$ depends on two variables z and φ. It can be derived that this function satisfies two LMBW-type equations,

$$\frac{\partial}{\partial z}\ln\rho(z,\varphi)=\frac{1}{k_BT}\frac{\partial}{\partial z}[B(z)\cos\varphi]+\int_{-\infty}^{\infty}dz'\int_0^{2\pi}d\varphi'\int_0^{\infty}qdqc(q,z,z',\varphi,\varphi')\times\frac{\partial\rho(z',\varphi')}{\partial z'} \tag{6}$$

and

$$\frac{\partial}{\partial\varphi}\ln\rho(z,\varphi)=\frac{1}{k_BT}\frac{\partial}{\partial\varphi}[B(z)\cos\varphi]+\int_{-\infty}^{\infty}dz'\int_0^{2\pi}d\varphi'\int_0^{\infty}qdqc(q,z,z',\varphi,\varphi')\times\frac{\partial\rho(z',\varphi')}{\partial\varphi'}, \tag{7}$$

which take into account both the inhomogeneity and anisotropy of $\rho(z,\varphi)$. Equations (6) and (7) represent the generalization of the usual LMBW approach to the anisotropic inhomogeneous case. For $\partial/\partial z\equiv 0$ or $\partial/\partial\varphi\equiv 0$ these equations reduce to those well known for homogeneous anisotropic or inhomogeneous isotropic systems, respectively [5,6,44–46].

The LMBW and IAOZ equations are exact but should be closed to connect the total and direct correlation functions. The most general form of such a closure is

$$h(q,z_1,z_2,\varphi_1,\varphi_2)=\exp\left(-\frac{u(r_{12},\varphi_1,\varphi_2)}{k_BT}+h(q,z_1,z_2,\varphi_1,\varphi_2)-c(q,z_1,z_2,\varphi_1,\varphi_2)+b(q,z_1,z_2,\varphi_1,\varphi_2)\right)-1, \tag{8}$$

where $u(r_{12},\varphi_1,\varphi_2)=\phi(r_{12})-J(r_{12})\cos(\varphi_1-\varphi_2)$ is the interparticle potential of the interactions, $b(q,z_1,z_2,\varphi_1,\varphi_2)$ denotes the bridge function and $r_{12}=[q^2+(z_1-z_2)^2]^{1/2}$. The bridge function cannot be determined exactly within any theory and the standard practice is to approximate it. One of the ways is to use a soft mean spherical approximation (SMSA) [44,45,48,51,52]. In the inhomogeneous anisotropic case it can be cast in the form

$$b(q,z_1,z_2,\varphi_1,\varphi_2)=\ln[1+\tau(q,z_1,z_2,\varphi_1,\varphi_2)]-\tau(q,z_1,z_2,\varphi_1,\varphi_2), \tag{9}$$

where

$$\tau(q,z_1,z_2,\varphi_1,\varphi_2)=h(q,z_1,z_2,\varphi_1,\varphi_2)-c(q,z_1,z_2,\varphi_1,\varphi_2)-\beta u_L(q,z_1,z_2,\varphi_1,\varphi_2) \tag{10}$$

is the renormalized indirect correlation function and $\beta=1/(k_BT)$ the inverse Kelvin temperature with k_B being the Boltzmann's constant. The long-ranged part u_L can be extracted [44,45,48] from the total potential u using the Boltzmann-like switching exponent built on the soft-core potential as $u_L(q,z_1,z_2,\varphi_1,\varphi_2)=-J(r_{12})\cos(\varphi_1-\varphi_2)\exp[-\beta\phi(r_{12})]$.

Equations (5)–(8) constitute a very complicated set of coupled IAOZ-LMBW-SMSA nonlinear integro-differential equations with respect to the functions h, c, and ρ. The main problem in solving of these equations is the fact that the unknown functions $h(q,z_1,z_2,\varphi_1,\varphi_2)$ and $c(q,z_1,z_2,\varphi_1,\varphi_2)$ depend on up to five (three spatial and two angle) variables (instead of one spatial coordinate r_{12} as in the case of simple homogeneous isotropic liquids). In addition it is necessary to perform cumbersome multidimensional integrations on the right-hand side of the IAOZ equation. This complicates the calculations drastically and leads to unresolvable numerical difficulties.

C. Inhomogeneous angle-harmonics expansion formalism

A method to remedy such a situation is based on an inhomogeneous angle-harmonics expansion formalism. The main idea lies in the fact that at any given values of q, z_1, and z_2, the two-body correlation functions $\{h,c\}\equiv f(q,z_1,z_2,\varphi_1,\varphi_2)$ are periodic in the two angle variables φ_1 and φ_2. Thus they readily can be expanded in sine and cosine harmonics as

$$f(q,z_1,z_2,\varphi_1,\varphi_2)=\sum_{n,m=0}^{\infty}\sum_{l,l'=0,1}f_{nmll'}(q,z_1,z_2)T_{nl}(\varphi_1)T_{ml'}(\varphi_2) \tag{11}$$

using the orthogonal Chebyshev polynomials

$$T_{n0}(\varphi)=\cos(n\varphi),$$

$$T_{n1}(\varphi)=-\frac{1}{n}\frac{dT_{n0}(\varphi)}{d\varphi}=\sin(n\varphi). \tag{12}$$

In our case $f_{nmll'}=f_{nml}\delta_{ll'}$, because the two-body correlation functions are invariant with respect to the transformation $(\varphi_1,\varphi_2)\leftrightarrow(-\varphi_1,-\varphi_2)$ in view of the symmetry of Hamiltonian (1). Then exploiting the orthonormality condition

$$\int_0^{2\pi}T_{nl}(\varphi)T_{ml'}(\varphi)d\varphi=t_n\delta_{nm}\delta_{ll'}, \tag{13}$$

where $t_n=\pi(1-\delta_{n0})+2\pi\delta_{n0}$, yields the expansion coefficients

$$f_{nml}(q,z_1,z_2)=\frac{1}{t_nt_m}\int_0^{2\pi}\int_0^{2\pi}d\varphi_1d\varphi_2f(q,z_1,z_2,\varphi_1,\varphi_2)T_{nl}(\varphi_1)\times T_{ml}(\varphi_2) \tag{14}$$

for the two-body correlation functions.

In terms of the above expansion coefficients, the IAOZ equation (5) can be reduced to the form

$$h_{nml}(q,z_1,z_2)=c_{nml}(q,z_1,z_2)+\sum_{n',m'=0}^{\infty}\int_Q d\mathbf{q}'\int_{-\infty}^{\infty}dz_3\times c_{nm'l}(|\mathbf{q}-\mathbf{q}'|,z_1,z_3)\times\rho_{n'm'l}(z_3)h_{n'ml}(q',z_3,z_2), \tag{15}$$

where $\{h,c\}_{nml}\equiv f_{nml}(q,z_1,z_2)$ and

$$\rho_{nml}(z) = \frac{1}{2\pi}\int_0^{2\pi} \rho(z,\varphi) T_{nl}(\varphi) T_{ml}(\varphi) d\varphi \tag{16}$$

are the angle moments of $\rho(z,\varphi)$. The matrix representation (15) looks like the IOZ equation corresponding to a mixture of isotropic inhomogeneous fluids. This is a very nice property because the problem can now be solved by adapting approaches already known for isotropic systems.

The polynomial expansion of the inhomogeneous anisotropic one-body density function $\rho(z,\varphi)$ can be performed in a similar way. Taking into account that this function at each given z is periodic with respect to φ one obtains

$$\rho(z,\varphi) = \exp\left(\beta B(z)\cos\varphi + \sum_{n=0}^{\infty} a_n(z) T_{n0}(\varphi)\right), \tag{17}$$

where $a_n(z)$ are the expansion coefficients, and only cosine harmonics should be included due to the property $\rho(z,-\varphi)=\rho(z,\varphi)$. Then the cumbersome LMBW equations (6) and (7) simplify significantly, because the integration over angle variables can now be performed analytically. Indeed, substituting the one-body expansion [Eq. (17)] into the first LMBW equation [Eq. (6)], multiplying both sides of this equation by the polynomials $T_{n0}(\varphi)$ (with $n=0,1,2,\ldots$) and integrating in φ yields the following set of integro-differential equations with respect to the expansion coefficients:

$$\frac{da_n(z)}{dz} = \int_{-\infty}^{\infty} dz' \sum_{m=0}^{\infty} G_{nm}(z,z') \frac{da_m(z')}{dz'}, \tag{18}$$

where

$$G_{nm}(z,z') = \sum_{m'=0}^{\infty} c_{nm'0}(z,z') \rho_{m'm0}(z') \tag{19}$$

are the kernels and

$$c_{nm'0}(z,z') = 2\pi \int_0^{\infty} q dq c_{nm'0}(q,z,z') \tag{20}$$

being the expansion coefficients for the direct correlation function integrated along the interface. The result for the second LMBW equation is

$$a_n(z) = \frac{2\pi}{n} \sum_{m=1}^{\infty} m \int_0^{\infty} q dq \int_{-\infty}^{\infty} dz' c_{nm1}(q,z,z') \rho_{m00}(z'), \tag{21}$$

where $n \geqslant 1$.

The inhomogeneous particle number density $\rho(z)$ is obtained by averaging the orientation-dependent distribution function

$$\rho(z) = \frac{1}{2\pi}\int_0^{2\pi} \rho(z,\varphi) d\varphi \equiv \rho_{000}(z) \tag{22}$$

that represents the zeroth moment [Eq. (16)] of $\rho(z,\varphi)$. The inhomogeneous magnetization $\mathcal{M}(z)$ appears by involving the next moments as

$$\mathcal{M}(z) = \frac{1}{2\pi}\int_0^{2\pi} \frac{\rho(z,\varphi)}{\rho(z)} \cos\varphi d\varphi \equiv \frac{\rho_{010}(z)}{\rho_{000}(z)} = \frac{\rho_{100}(z)}{\rho_{000}(z)}. \tag{23}$$

Note that the zeroth-order coefficient a_0 in Eq. (17) can be expressed in terms of $\rho(z)$ and the remaining $(n=1,2,\ldots)$ coefficients a_n as

$$a_0(z) = \ln \frac{\rho(z)}{\frac{1}{2\pi}\int_0^{2\pi} \exp\left(\beta B(z)\cos\varphi + \sum_{n=1}^{\infty} a_n(z) T_{n0}(\varphi)\right) d\varphi}. \tag{24}$$

On the other hand, the magnetization in view of Eq. (23) does not depend on a_0 (it depends on a_n with $n=1,2,\ldots$).

The angle-harmonics expansion formalism proposed can be applied to XY-spin systems with arbitrary regular anisotropic potentials. An important feature of this approach is that the expansion coefficients for the correlation functions rapidly tend to zero with increasing the number $\mathcal{N}$ of harmonics. It follows from the quick vanishing of the harmonics coefficients for regular anisotropic potentials. Moreover, the logarithmic form $\ln\rho(z,\varphi)$ for the expansion [see Eq. (17)] of $\rho(z,\varphi)$ automatically provides the correct dependence on the external field [such a dependence results from the LMBW equations, Eqs. (6) and (7)] and additionally speeds up the convergence. Thus, only a finite number $\mathcal{N}$ of harmonics should be in fact involved in the computations. In other words, the infinite upper limit for subscripts in Eqs. (15), (17), (18), (21), and (24) should be replaced by a finite number. The actual value of $\mathcal{N}$ will depend on the form of the anisotropic potential. For instance, in the case of the simplest XY-spin fluid model considered [Eq. (1)], the anisotropic interparticle potential $u(r,\varphi_1,\varphi_2)=\phi(r)-J(r)\cos(\varphi_1-\varphi_2)$ can be expanded in terms of zeroth and first harmonics exclusively, because of $\cos(\varphi_1-\varphi_2)=T_{10}(\varphi_1)T_{10}(\varphi_2)+T_{11}(\varphi_1)T_{11}(\varphi_2)$. The number $\mathcal{N}$ of harmonics for the correlation functions will be slightly larger $(\mathcal{N}>1)$ due to the exponential nonlinearity (anharmonicity) in the anisotropic interaction of the SMSA closure. The computations show (see Sec. III) that the condition $\mathcal{N}\gtrsim 2$ is quite enough to obtain reliable results. Note that the anharmonicity appears in view of the specific long-ranged separation $u_L(q,z_1,z_2,\varphi_1,\varphi_2)=-J(r_{12})\cos(\varphi_1-\varphi_2)\exp[-\beta\phi(r_{12})]$ for which the SMSA closure [Eqs. (8)–(10)] can be rewritten in the form $h=(1+h-c-\beta u_L)\exp(-\beta\phi)\exp\{\beta J\cos(\varphi_1-\varphi_2)[1-\exp(-\beta\phi)]\}-1$. Taking into account that the soft-repulsion potential $\phi(r)$ is nonzero at $r_{12}<2^{1/6}\sigma$ [see Eq. (3)] yields the exponential nonlinearity in angle variables.

Handling the SMSA closure also presents no difficulties, because for distances $r_{12}\geqslant 2^{1/6}\sigma$ [where $\phi(r_{12})=0$] we have from Eqs. (8)–(10) that $c(q,z_1,z_2,\varphi_1,\varphi_2)=\beta J(r_{12})\cos(\varphi_1-\varphi_2)$. Then one finds $c_{110}(q,z_1,z_2)=c_{111}(q,z_1,z_2)=\beta J(r_{12})$, while all other c coefficients will be equal to zero at $r_{12}\geqslant 2^{1/6}\sigma$. Only for $r_{12}<2^{1/6}\sigma$, we should perform a numerical integration over angle variables [according to Eq. (14)] of

the right-hand side of Eq. (8) in order to get the expansion coefficients $h_{nml}(q,z_1,z_2)$ and $c_{nml}(q,z_1,z_2)$ for higher-order $(n,m>1)$ harmonics.

D. Interpolation of the inhomogeneity in the anisotropic direct correlation functions

Despite the obvious simplifications obtained within the inhomogeneous angle-harmonics formalism, the set of IOZ-like equations [Eq. (15)] for the two-body correlation functions still remains too cumbersome to be handled directly. For this reason, it is quite reasonable to solve explicitly the LMBW equations [Eqs. (18) and (21)] for the one-body distribution function $\rho(z,\varphi)$, while the expansion coefficients $c_{nml}(q,z_1,z_2)$ of the inhomogeneous direct correlation function $c(q,z_1,z_2,\varphi_1,\varphi_2)$ can be consistently interpolated between the bulk functions obtained from the homogeneous but anisotropic AOZ-SMSA approach.

The most efficient interpolating scheme can be built as follows. First, the inhomogeneous anisotropic direct correlation function is presented by averaging its homogeneous anisotropic counterparts evaluated at densities $\rho(z)$ corresponding to two given positions z_1 and z_2 on the interface, i.e.,

$$c(q,z_1,z_2,\varphi_1,\varphi_2) = \tfrac{1}{2}\{c[r_{12},\varphi_1,\varphi_2;\rho(z_1)] + c[r_{12},\varphi_1,\varphi_2;\rho(z_2)]\}, \tag{25}$$

where $r_{12}=[q^2+(z_1-z_2)^2]^{1/2}$. The approximation given by Eq. (25) is quite natural, because in the limit of a weak spatial inhomogeneity it becomes exact. Performing the angular harmonics expansion [Eq. (11)] of $c(q,z_1,z_2,\varphi_1,\varphi_2)$ and $c(r_{12},\varphi_1,\varphi_2;\rho)$ one obtains from Eq. (25) that

$$c_{nml}(q,z_1,z_2) = \tfrac{1}{2}\{c_{nml}[r_{12};\rho(z_1)] + c_{nml}[r_{12};\rho(z_2)]\}. \tag{26}$$

In its turn, the homogeneous anisotropic function $c[r_{12},\varphi_1,\varphi_2;\rho(z)]$ or its expansion coefficients $c_{nml}[r_{12};\rho(z)]$ can be nonlinearly interpolated for any $\rho(z)\in[\rho_1,\rho_2]$ as

$$c[r_{12},\varphi_1,\varphi_2;\rho(z)] = \sum_{k=1,2}\sum_{p=0,1}\omega_k^{(p)}[\rho(z)]c^{(p)}(r_{12},\varphi_1,\varphi_2;\rho_k) \tag{27}$$

or

$$c_{nml}[r_{12};\rho(z)] = \sum_{k=1,2}\sum_{p=0,1}\omega_k^{(p)}[\rho(z)]c_{nml}^{(p)}(r_{12};\rho_k), \tag{28}$$

respectively, using the values of $c\equiv c^{(0)}$ and $c_{nml}\equiv c_{nml}^{(0)}$ as well as the p-fold density derivatives $c^{(p)}=\partial^p c/\partial\rho^p$ and $c_{nml}^{(p)}=\partial^p c_{nml}/\partial\rho^p$ at only two values of $\rho=\rho_1$ and $\rho=\rho_2$ which relate to the bulk gas and liquid phases, respectively $(\rho_1<\rho_2)$. The ρ-dependent coefficients $\omega_k^{(p)}(\rho)$ are chosen in such a way to provide the coexistence of the genuine and interpolated functions as well as their density derivatives up to a given order at the boundaries of the interval $[\rho_1,\rho_2]$. Equation (28) is formally exact provided that an infinite number of terms $(p=0,1,\ldots,\infty)$ is included in the interpolation. In practice it is convenient to deal with a finite-order interpolation, for instance, with the well-recognized cubic interpolation. In the case of the cubic interpolation, when $p=0,1$ in Eq. (28), the ω coefficients are

$$\omega_1^{(0)}(\rho) = 1-3\chi+2\chi^3, \quad \omega_2^{(0)}(\rho) = 1-\omega_1^{(0)}(\rho),$$
$$\omega_1^{(1)}(\rho) = (\chi-2\chi^2+\chi^3)\Delta\rho, \quad \omega_2^{(1)}(\rho) = -\omega_1^{(1)}(\rho)\big|_{\chi=1-\chi}, \tag{29}$$

where $\chi=(\rho-\rho_1)/\Delta\rho$ and $\Delta\rho=\rho_2-\rho_1$. Then the original and interpolated functions as well as their first-order density derivatives will coincide at the boundary values $\rho=\rho_1$ and $\rho=\rho_2$.

Higher-order terms can be taken into account effectively by modifying the interpolation coefficients [39]. The simplest form of such a modification is

$$\tilde{\omega}_1^{(0)}(\rho) = \omega_1^{(0)}(\rho) + \alpha\omega_1^{(0)^2}[1-\omega_1^{(0)}(\rho)]^2,$$
$$\tilde{\omega}_2^{(0)}(\rho) = \omega_2^{(0)}(\rho) - \alpha\omega_2^{(0)^2}[1-\omega_2^{(0)}(\rho)]^2 = 1-\tilde{\omega}_1^{(0)}(\rho), \tag{30}$$

and

$$\tilde{\omega}_1^{(1)}(\rho) = \omega_1^{(1)}(\rho) + \alpha'\omega_1^{(1)^2},$$
$$\tilde{\omega}_2^{(1)}(\rho) = \omega_2^{(1)}(\rho) - \alpha'\omega_2^{(1)^2} = -\tilde{\omega}_1^{(1)}(\rho)\big|_{\chi=1-\chi}, \tag{31}$$

where α and α' are the parameters to be determined from self-consistent conditions (see Sec. II F below). The difference in the modification forms for $\omega_{1,2}^{(0)}$ and $\omega_{1,2}^{(1)}$ is caused by the fact that $\omega_{1,2}^{(0)}$ take the values 0 or 1 on the boundaries of the interval $[\rho_1,\rho_2]$, while $\omega_{1,2}^{(1)}$ are equal to zero at $\rho=\rho_1$ and $\rho=\rho_2$. The modified terms quadratically vanish as $\omega_k^{(0)}\to 1$ or $\omega_k^{(0)}\to 0$ as well as $\omega_k^{(1)}\to 0$ when approaching the bulk gas $(k=1)$ or liquid $(k=2)$ phases. Therefore, the modification coefficients do not distort the values of $c(r_{12},\varphi_1,\varphi_2;\rho)$ and its first derivative $c^{(1)}(r_{12},\varphi_1,\varphi_2;\rho)$ at the reference densities $\rho=\rho_k$, where $k=1,2$. The modifications are maximal in the metastable region when the local density $\rho(z)$ deviates most from ρ_1 and ρ_2. Then, for instance, $\omega_{1,2}^{(0)}\sim 1-\omega_{1,2}^{(0)}\sim 1/2$, and the deviations between $\tilde{\omega}_{1,2}^{(0)}$ and $\omega_{1,2}^{(0)}$ achieve a maximum of $\alpha/16$.

In view of Eqs. (26)–(31), the resulting interpolation reads as

$$c_{nml}(q,z_1,z_2) = \frac{1}{2}\sum_{k=1,2}\sum_{p=0,1}\{\tilde{\omega}_k^{(p)}[\rho_\sigma(z_1)] + \tilde{\omega}_k^{(p)}[\rho_\sigma(z_2)]\} \times c_{nml}^{(p)}(r_{12};\rho_k). \tag{32}$$

Note that the interpolation coefficients $\tilde{\omega}_k^{(p)}[\rho_\sigma(z)]$ should be calculated at the averaged coarse-grained density

$$\rho_\sigma(z) = \frac{1}{\sigma}\int_{z-\sigma/2}^{z+\sigma/2}\rho(z')dz' \tag{33}$$

to take into account the influence of the size of the particle.

E. Bulk anisotropic correlation functions

The harmonics coefficients $c_{nml}(r;\rho)$ for the homogeneous anisotropic direct correlation function $c(r,\varphi_1,\varphi_2;\rho)$

can be found at a given bulk density ρ from the homogeneous anisotropic Ornstein-Zernike-like equations in conjunction with the homogeneous anisotropic SMSA closure [44,45]. The latter is obtained from the inhomogeneous anisotropic SMSA closure [Eqs. (8)–(10)] by formal replacement of (q,z_1,z_2) by r. The homogeneous anisotropic integral equations can be obtained from the IAOZ ones [Eq. (15)] by replacing (q,z_1,z_2) by r and $\rho(z,\varphi)$ by $\rho\xi(\varphi;\rho)$. This yields

$$h_{nml}(p;\rho) = c_{nml}(p;\rho) + \rho \sum_{n',m'=0}^{\mathcal{N}} c_{nm'l}(p;\rho)\xi_{n'm'l}(\rho)h_{n'ml}(p;\rho), \tag{34}$$

where the three-dimensional (3D) spatial Fourier transform

$$f(p) = \int_V f(r)\exp(i\mathbf{p}\cdot\mathbf{r})d\mathbf{r}$$

has been used. Here

$$\xi_{nml}(\rho) = \frac{1}{2\pi}\int_0^{2\pi} \xi(\varphi;\rho)T_{nl}(\varphi)T_{ml}(\varphi)d\varphi \tag{35}$$

are the moments of the bulk one-body distribution function

$$\xi(\varphi;\rho) = Z^{-1}(\rho)\exp\left(\beta B\cos\varphi + \sum_{n=1}^{\mathcal{N}} a_n(\rho)T_{n0}(\varphi)\right) \tag{36}$$

with

$$Z(\rho) = \frac{1}{2\pi}\int_0^{2\pi} \exp\left(\beta B\cos\varphi + \sum_{n=1}^{\mathcal{N}} a_n(\rho)T_{n0}(\varphi)\right)d\varphi$$

being determined from the normalization condition $\frac{1}{2\pi}\int_0^{2\pi}\xi(\varphi;\rho)d\varphi=1$ and a homogeneous external field $B(z) \equiv B$ has been considered. The expansion coefficients a_n can be found from the LMBW equation [Eq. (7)] in the bulk limit $(q,z_1,z_2)\to r$, where $\partial/\partial z=0$. Then one obtains from Eq. (21) that

$$a_n(\rho) = \frac{4\pi\rho}{n}\sum_{m=1}^{\mathcal{N}} m\xi_{m00}(\rho)\int_0^{\infty} c_{nm1}(r;\rho)r^2dr = \frac{\rho}{n}\sum_{m=1}^{\mathcal{N}} m\xi_{m00}(\rho)c_{nm1}(p=0;\rho). \tag{37}$$

The coupled set of equations [Eqs. (34) and (37)] complimented by the homogeneous SMSA closure can now be easily solved with respect to $c_{nml}(r;\rho)$, $h_{nml}(r;\rho)$, and $a_n(\rho)$ because it represents in fact a system of nonlinear but algebraic relations. The coexisting bulk gas ρ_1 and liquid ρ_2 densities can be determined at given values of T and B from the mechanical and chemical equilibrium conditions

$$P(\rho_1,T,B) = P(\rho_2,T,B),$$

$$\mu(\rho_1,T,B) = \mu(\rho_2,T,B). \tag{38}$$

The pressure P can readily be calculated using the virial equation of state [44,45]

$$\frac{\beta P}{\rho} = 1 - \frac{1}{6}\frac{\beta\rho}{(2\pi)^2}\int d\mathbf{r}d\varphi_1 d\varphi_2 \xi(\varphi_1;\rho)\xi(\varphi_2;\rho)g(r,\varphi_1,\varphi_2;\rho)r \times\frac{du(r,\varphi_1,\varphi_2)}{dr} = 1 - \frac{2\pi\beta\rho}{3}\sum_{n,m=0}^{\mathcal{N}}\int_0^{\infty} r^3dr\left(\frac{d\phi(r)}{dr}\xi_{n00}(\rho)\xi_{m00}(\rho)g_{nm0}(r;\rho) - \frac{dJ(r)}{dr}\sum_{l=0,1}\xi_{n1l}(\rho)\xi_{m1l}(\rho)g_{nml}(r;\rho)\right), \tag{39}$$

where $g(r,\varphi_1,\varphi_2;\rho)=h(r,\varphi_1,\varphi_2;\rho)+1$ is the radial distribution function and $g_{nml}(r;\rho)$ its harmonics coefficients. The chemical potential μ can be evaluated by integrating the thermodynamic relation $\rho\beta(\partial\mu^*/\partial\rho)_{T,B}=\beta(\partial P/\partial\rho)_{T,B}-1$, where μ^* is the excess part of μ. Then the second line of Eq. (38) can be replaced by the Maxwell construction

$$\left(\frac{1}{\rho_1}-\frac{1}{\rho_2}\right)\mathcal{P} + \int_{\rho_1}^{\rho_2} P(\rho,T,B)\frac{d\rho}{\rho^2} = 0, \tag{40}$$

where $\mathcal{P}$ denotes the coexistence pressure.

Having the coexisting densities ρ_1 and ρ_2, the harmonics coefficients $c_{nml}(r;\rho_k)$ as well as $a_n^{(k)}\equiv a_n(\rho_k)$ can be found by solving the homogeneous anisotropic AOZ-LMBW equations [Eqs. (34) and (37)] two times ($k=1$ and 2), namely, at $\rho=\rho_1$ and $\rho=\rho_2$. The density derivatives $c_{nml}^{(1)}(r;\rho_k) = [c_{nml}(r;\rho_k+\delta\rho)-c_{nml}(r;\rho_k)]/\delta\rho$ can by evaluated numerically by recalculating the AOZ-LMBW equations at shifted densities $\rho_k+\delta\rho$ with an increment of $\delta\rho \ll (\rho_2-\rho_1)$.

F. Solving the LMBW equations

In view of the finite number of harmonics and the interpolation used [Eq. (32)], the first LMBW equation [Eq. (18)] takes now the form

$$\frac{da_n(z)}{dz} = \int_{-\infty}^{\infty} dz' \sum_{m=0}^{\mathcal{N}} G_{nm}(z,z')\frac{da_m(z')}{dz'} \tag{41}$$

at $n=0,1,2,\ldots,\mathcal{N}$, where

$$G_{nm}(z,z') = \frac{1}{2}\sum_{m'=0}^{\mathcal{N}}\sum_{k=1,2}\sum_{p=0,1}\{\tilde{\omega}_k^{(p)}[\rho_\sigma(z)] + \tilde{\omega}_k^{(p)}[\rho_\sigma(z')]\} \times c_{nm'0}^{(p)}(|z-z'|;\rho_k)\rho_{m'm0}(z') \tag{42}$$

are the kernels,

$$c_{nm'0}^{(p)}(|z_1-z_2|;\rho_k) = 2\pi\int qdqc_{nm'0}^{(p)}([q^2+(z_1-z_2)^2]^{1/2};\rho_k) \tag{43}$$

denote the expansion coefficients for the direct correlation integrated with respect to the plane vector $\mathbf{q}$, and

$$\rho_{nml}(z) = \frac{1}{2\pi}\int_0^{2\pi} \rho(z,\varphi)T_{nl}(\varphi)T_{ml}(\varphi)d\varphi$$
$$= \frac{1}{2\pi}\int_0^{2\pi} \exp\left(\beta B\cos\varphi + \sum_{n=0}^{\mathcal{N}} a_n(z)T_{n0}(\varphi)\right)$$
$$\times T_{nl}(\varphi)T_{ml}(\varphi)d\varphi \tag{44}$$

are the one-body distribution moments. Equation (41) represents the set of $(\mathcal{N}+1)$ coupled nonlinear integro-differential equations with respect to the same number of unknown functions $a_0(z), a_1(z), a_2(z), \ldots, a_{\mathcal{N}}(z)$.

As any other differential equations involving derivatives, the integro-differential LMBW equation [Eq. (41)] requires the knowledge of $(\mathcal{N}+1)$ initial conditions to be solved uniquely. The first condition can be introduced by fixing the value of the particle number density at the origin of the coordinate system,

$$\rho(z)|_{z=0} = \rho_{000}(z)|_{z=0} = \rho_0. \tag{45}$$

The choice of ρ_0 is to some extent arbitrary, because different values of ρ_0 will merely correspond to shifting the coordinate frame along axis z. In other words, if $[a_n(z)]$ is a solution to the LMBW equation [Eq. (41)], the shifted profiles $[a_n(z+\Delta)]$ will also satisfy this equation in the presence of an external field $B(z+\Delta)=B(z)$ for any finite Δ as this follows from the structure of Eqs. (41)–(44). Note however that ρ_0 should lie in the interval $]\rho_1,\rho_2[$ to provide the existence of desired nontrivial solutions $[a_n(z)\neq \text{const}]$ to the LMBW equation. Choosing ρ_0 outside this interval, we can come to a situation with no solution or with only the trivial solutions $a_n(z)=\text{const}$.

The $\mathcal{N}$ remaining integration constants specify the values of $a_n(z)$ (where $n=1,2,\ldots,\mathcal{N}$) at the chosen coordinate origin, i.e.,

$$a_n(z)|_{z=0} = a_n(0). \tag{46}$$

The quantities $a_n(0)$ should be chosen in such a way as to provide the coincidence of the asymptotic values $a_n(z\to-\infty)$ and $a_n(z\to+\infty)$ of the obtained solution $a_n(z)$ to the first LMBW equation [Eq. (41)] with the bulk values $a_n^{(1)}=a_n(\rho_1)$ and $a_n^{(2)}=a_n(\rho_2)$ already known from the solution [Eq. (37)] to the second LMBW equation [Eq. (7)] in the bulk limit. For instance, fulfilling the equality $a_n(z\to-\infty)=a_n^{(1)}$ far left from the interface in the bulk gas phase, the asymptotic value $a_n(z\to+\infty)$ of $a_n(z)$ far right from the interface in the bulk liquid phase will be the result of the inhomogeneous LMBW integration [Eq. (41)], and vice versa. Then the second equality $a_n(z\to+\infty)=a_n^{(2)}$ will be satisfied automatically, provided the problem is solved exactly.

The values $\lim_{z\to-\infty}\rho(z)$ and $\lim_{z\to+\infty}\rho(z)$, found from the asymptotics of the inhomogeneous anisotropic LMBW solution $\rho(z)$, should coincide with the bulk values ρ_1 and ρ_2 obtained within the homogeneous AOZ-LMBW-SMSA approach [Eqs. (34) and (37)] from the equilibrium conditions [Eq. (38)]. This follows from the fact that the LMBW equations satisfy the variational principle for the free energy and thus implicitly provide the mechanical and chemical balance between the coexistence phases. Note however that the LMBW equations are integrated approximately because of the approximate character of the interpolation used for the inhomogeneous direct correlation function [Eq. (32)]. Moreover, the bulk correlation functions obtained within the homogeneous AOZ-LMBW-SMSA approach [Eqs. (34) and (37)] are also not exact because of the approximate form of the SMSA closure. For this reason, the asymptotic and bulk values of ρ may, generally speaking, differ to a greater or lesser extent. For the same reason, the equality $a_n(z\to\mp\infty)=a_n^{(1,2)}$ with $n\geqslant 1$ cannot be satisfied exactly in two bulk phases simultaneously by varying only one parameter $a_n(0)$ [Eq. (46)].

The internal consistency between the asymptotic LMBW and bulk AOZ-SMSA values can be achieved by optimizing the parameters α and α' of the interpolation [Eqs. (30)–(32)] to fulfill the self-consistent conditions

$$\lim_{z\to-\infty}\rho(z)=\rho_1, \quad \lim_{z\to+\infty}\rho(z)=\rho_2. \tag{47}$$

The full consistency, when $a_n(z\to\mp\infty)=a_n^{(1,2)}$ for any $n=0,1,2,\ldots,\mathcal{N}$, can be reached by extending the set of interpolation parameters. In particular, this can be done by choosing different values of α and α' for different harmonics coefficients c_{nml}. However, as will be shown in actual calculations, the optimization of only one interpolation parameter α (with $\alpha'\equiv 0$) allows to achieve a very good consistency for all the functions $a_n(z)$.

G. Surface tension

The surface tension can be evaluated using the Triezenberg and Zwanzig formula [53] which in the case of planar liquid-vapor interfaces for anisotropic systems reads as

$$\gamma = \frac{k_BT}{4}\left(\frac{1}{2\pi}\right)^2\int_{-\infty}^{\infty}dz_1\int_{-\infty}^{\infty}dz_2\int_0^{2\pi}d\varphi_1\int_0^{2\pi}d\varphi_2\int_0^{\infty}dq$$
$$\times\frac{\partial\rho(z_1,\varphi_1)}{\partial z_1}\frac{\partial\rho(z_2,\varphi_2)}{\partial z_2}2\pi q^3 c(q,z_1,z_2,\varphi_1,\varphi_2). \tag{48}$$

Taking into account the harmonics expansions of $c(q,z_1,z_2,\varphi_1,\varphi_2)$ [Eq. (14)] and $\rho(z,\varphi)$ [Eq. (17)], the surface tension coefficient can be cast in the form

$$\gamma = \frac{k_BT}{4}\int_{-\infty}^{\infty}dz_1\int_{-\infty}^{\infty}dz_2\sum_{n,m=0}^{\mathcal{N}}\sum_{n',m'=0}^{\mathcal{N}}\rho_{nn'0}(z_1)$$
$$\times\frac{da_n(z_1)}{dz_1}\rho_{mm'0}(z_2)\frac{da_m(z_2)}{dz_2}\Gamma_{n'm'0}(z_1,z_2), \tag{49}$$

where, in view of the interpolation of the direct correlation function,

$$\Gamma_{nm}(z_1,z_2) = \frac{1}{2}\sum_{k=1,2}\sum_{p=0,1}\{\tilde{\omega}_k^{(p)}[\rho_\sigma(z_1)]+\tilde{\omega}_k^{(p)}[\rho_\sigma(z_2)]\}$$
$$\times C_{nm0}^{(p)}(|z_1-z_2|;\rho_k) \tag{50}$$

and

$$C^{(p)}_{nm0}(|z_1-z_2|;\rho_k)=2\pi\int q^3dqc^{(p)}_{nm0}([q^2+(z_1-z_2)^2]^{1/2};\rho_k). \tag{51}$$

Note that the one-dimensional integration in Eq. (51) can be performed in advance because of the interpolation, so that the overall dimension of the integration in Eq. (49) does not increase. In such a way, the five-dimensional integration [Eq. (48)] has been reduced to the two-dimensional one [Eq. (49)] with the sums over $(\mathcal{N}+1)^4$ harmonics terms.

III. NUMERICAL RESULTS

A. Algorithm and computational details

Since the spatial derivative profiles $a'_n(z)=da_n(z)/dz$ vanish far $(z\to\pm\infty)$ from the interfaces and the kernel functions $G_{nm}(z,z')$ tend to zero with increasing $|z-z'|$, the set of LMBW equations [Eq. (41)] can be discretized on a finite interval $-L/2\leqslant z\leqslant L/2$. The length $L\gg\sigma$ should be sufficiently large to be entitled to neglect the truncation terms $a'_n(z)|_{z=\pm L/2}\approx 0$ and $c^{(p)}_{nml}(L;\rho_k)\approx 0$. Using the uniformly distributed points $z_l\in[-L/2,L/2]$ with $l=1,2,\ldots,\mathcal{L}$ and $\mathcal{L}\gg 1$, the discrete version of the LMBW equations can be cast in the compact matrix form $[\mathbf{I}-\mathbf{G}]\mathbf{a}'=0$. Here $\mathbf{I}$ is the unit matrix, $\mathbf{a}'$ denotes the vector of grid values of $a'_n(z)$ at $z=z_l$, and $\mathbf{G}$ is the matrix with the elements $G_{nm}(z_l,z_{l'})L/(\mathcal{L}-1)$. In the limit $L,\mathcal{L}\to\infty$ provided $L/\mathcal{L}\to 0$, the discrete version turns into the continuous one.

The LMBW matrix equations together with the self-consistent AOZ-SMSA conditions were solved iteratively with respect to $a'_n(z_l)$ as well as $a_n(0)$ and α. Having derivatives $a'_n(z)$, the harmonics coefficient profiles were evaluated at given integration constants $a_n(0)$ as $a_n(z)=a_n(0)+\int_0^z a'_n(z')dz'$ applying the trapezoidal rule. The residuals to the LMBW equations and self-consistent conditions were evaluated for the current values of $a'_n(z_l)$, $a_n(0)$, and α. Using the residuals, these values were updated by tailoring the method of modified direct inversion in the iterative subspace (MDIIS) [54], and then iterated until they converged to a root-mean-square accuracy of 10^{-7}. In fact, the problem was reduced to solving a system of nonlinear equations with a great number of unknowns, $a'_n(z_l)$, $a_n(0)$, and α (interested readers are referred to Ref. [55], where the MDIIS algorithm is described in detail for the general case). We considered $L/2=40\sigma$ and $\mathcal{L}-1=2000$. The integration with respect to angle variables was carried out by Gauss-Chebyshev quadratures with the number of knots $\mathcal{K}=8$. The finite difference for the calculation of density derivatives was $\delta\rho^*=\delta\rho\sigma^3=0.001$. The number of harmonics involved was $\mathcal{N}+1=3$. Further increase of $\mathcal{K}$ and $\mathcal{N}$ as well as the grid resolution parameters L and $\mathcal{L}$ does not affect the solutions even in subcritical temperature regions.

The AOZ-SMSA equations [Eqs. (34) and (37)] were handled separately at the preparation stage before solving the LMBW equation [Eq. (41)]. The densities $\rho_{1,2}$ and harmonic coefficients $a_n^{(1,2)}$ of coexisting bulk anisotropic phases have been evaluated [from the equilibrium conditions, Eq. (38)] in the spirit of our previous papers [44,45] when considering homogeneous properties of the *XY* fluid. The harmonics coefficients of the direct correlation function have been integrated with respect to the lateral vector $\mathbf{q}$ [see Eq. (43)] in advance as well at two $(k=1,2)$ reference points using high-precision Gaussian quadratures.

The LMBW-AOZ-SMSA calculations were performed in the limit of a spatially homogeneous external magnetic field $dB(z)/dz=0$ when $B(z)\equiv B$. The dimensionless quantities $\rho^*(z)=\rho(z)\sigma^3$, $T^*=k_BT/\varepsilon$, $B^*=B/\varepsilon$, and $\gamma^*=\gamma\sigma^2/\varepsilon$ were chosen in the presentation of the results. We considered the following most characteristic values of the external field, $B^*=0$, 0.5, 2, 10, 40, and ∞.

The computations have shown that the best consistency of the results with a minimal correction of the interpolated direct correlation function [Eqs. (30)–(32)] when only one optimizing parameter α is used $(\alpha'=0)$ can be achieved as follows. First, the integration constants $a_n(0)$, where $n=1,2,\ldots,\mathcal{N}$ [see Eq. (46)], were chosen in such a way as to provide the exact coincidence of the asymptotic and bulk values of $a_n(z)$ in the gas phase, i.e., $\lim_{z\to-\infty}a_n(z)=a_n^{(1)}$. This automatically leads to the coincidence of the asymptotic and bulk gas magnetizations, i.e., $\lim_{z\to-\infty}\mathcal{M}(z)=\mathcal{M}_1\equiv\mathcal{M}(a_1^{(1)},a_2^{(1)},\ldots,a_{\mathcal{N}}^{(1)})$. Then the quantity $a_0(0)$ was obtained according to Eq. (24) by fixing the density profile $\rho(z=0)=\rho_0\in]\rho_1,\rho_2[$ at the origin of the coordinate system [see (Eq. (45)]. Finally, the parameter α of the self-consistency was optimized by requiring the exact coincidence of the asymptotic and bulk densities in the liquid phase, i.e., $\lim_{z\to+\infty}\rho(z)=\rho_2$.

It is worth to point out that for spatially homogeneous external fields, the first B term on the right-hand side of the first LMBW equation [Eq. (6)] vanishes since $dB(z)/dz=0$. The explicit external field contribution appears only in the second LMBW equation [Eq. (7)] and, as a result, in the expansion of the one-body density function [Eq. (17)]. No explicit B-terms enter into the equations for the expansion coefficients [Eqs. (18) and (21)], but they exist implicitly through the moments [Eq. (16)] of the one-body density function [Eq. (17)]. In addition, the external field contributes implicitly via the initial conditions [Eq. (46)] which involve the bulk values $a_n^{(1,2)}$. The latter are defined from the second LMBW equation in the bulk limit [see Eqs. (7), (21), and (37)] through the equilibrium conditions [Eq. (38)] and thus depend on B in a characteristic way.

Note also that instead of solving all $(n=0,1,2,\ldots)$ the integro-differential equations [see Eq. (41) or (18)] following from the first LMBW equality [Eq. (6)] we could alternatively use them only at $n=0$ and combine with the set $n=1,2,\ldots$ of integral equations for the expansion coefficients $a_n(z)$ obtained from the second LMBW relation [Eq. (7)]. Both ways are equivalent and should lead to identical results. Note however that we solve the equations numerically and discretize them to replace the infinite interval $z\in]-\infty,\infty[$ of the z integration by the finite one $[-L/2,L/2]$. Moreover, the spatial derivatives $da_m(z')/dz'$, which enter under the integrands in Eqs. (18) and (41), quickly decay to zero when moving away from the interfaces. This is contrary to the density moments $\rho_{m00}(z')$ which according to Eqs. (16) and (17) functionally depend on all $(m=0,1,2,\ldots)$ of the coefficients $a_m(z')$ and do not vanish for $z\to\pm\infty$. Therefore, the

integration over z' in the first set of equations [Eqs. (18) or (41)] can be restricted to a considerably smaller (z,z') domain in the two z dimensions, significantly reducing the computational expenses. At the same time, the second set of equations [Eq. (21)] is much more sensitive to the z-grid resolution and requires considerable larger domain sizes L.

B. LMBW solutions and consistency with bulk values

The density $\rho^*(z)$ and magnetization $\mathcal{M}(z)$ profiles at the liquid-vapor interfaces obtained within the LMBW-AOZ-SMSA approach for the XY fluid in the absence ($B=0$) and presence of the external magnetic fields $B^*=B/\varepsilon=0.5$, 2, 10, and 40 are plotted in subsets of Fig. 1 for several temperatures, $T^*=1.1$, 1.5, 1.9, and 2.2 up to subcritical values $T^*=2.3$, 2.4, or 2.5 in dependence on B. Note that at each given $B\neq 0$, the origin of the z-coordinate system was chosen in such a way as to provide the intersection of all the density profiles related to different temperatures T in the same point at $z=0$, i.e., $\rho(z=0,T,B)=\rho_0(B)$ [see Eq. (45)], where $\rho_0(B)\equiv\rho_c(B)$ is associated with the critical density. At $B=0$ we set $\rho_0^*=0.3$ for the sake of convenience. This nearly corresponds to the position of the center of the profile.

As can be seen, the density and magnetization profiles are monotonically increasing functions. At low enough temperatures, they are sufficiently sharp with large differences between the densities $\rho(\mp\infty)$ and magnetizations $\mathcal{M}(\mp\infty)$ corresponding to the bulk vapor ($z\to-\infty$) and bulk liquid ($z\to+\infty$) phases with $\rho(\infty)>\rho(-\infty)$ and $\mathcal{M}(\infty)>\mathcal{M}(-\infty)$. Here, the local values of $\rho(z)$ and $\mathcal{M}(z)$ quickly vary at the interface with changing z and tend to their bulk counterparts at $z\to\pm\infty$. Note that at $B=0$, the magnetization vanishes at $z\to-\infty$ for any temperature, i.e., $\mathcal{M}(-\infty)=0$, while $\mathcal{M}(\infty)\neq 0$ due to the spontaneous symmetry breaking. This means that in this case a transition between a paramagnetic gas and a ferromagnetic liquid takes place. In the presence of an external field, when $B\neq 0$ and $\mathcal{M}(\mp\infty)\neq 0$ because of the induced magnetization, we will observe a transition between a weakly magnetized gas and a strongly magnetized liquid $[\mathcal{M}(\infty)>\mathcal{M}(-\infty)]$. With increasing external field strength B, both asymptotic values $\mathcal{M}(\mp\infty)$ increase. The saturation regime, where the magnetizations $\mathcal{M}(\mp\infty)\approx 1$ almost reach the maximal possible value, is already found for $B^*\gtrsim 40$. On the other hand, the density profiles only vary slightly on the change of B. The interfaces become wider when approaching the critical point (ρ_c,T_c). At $T=T_c(B)$, the width of the interfaces goes to infinity (the interfaces are flat, see the horizontal dashed lines). For this reason we cannot come up to the critical temperature very closely, since then the interfacial width becomes too large and would exceed the fixed size L of the z domain considered. The values for the critical temperature T_c are written in Fig. 1 at the horizontal dashed lines. They were taken from our previous works [44,45] on homogeneous properties of the XY fluid. For higher temperatures $T>T_c(B)$, the liquid-vapor interfaces do not appear at all because of the dominance of temperature fluctuations over ferromagnetic interactions. This results in a homogeneous state with $\rho(z)=$const and $\mathcal{M}(z)=$const.

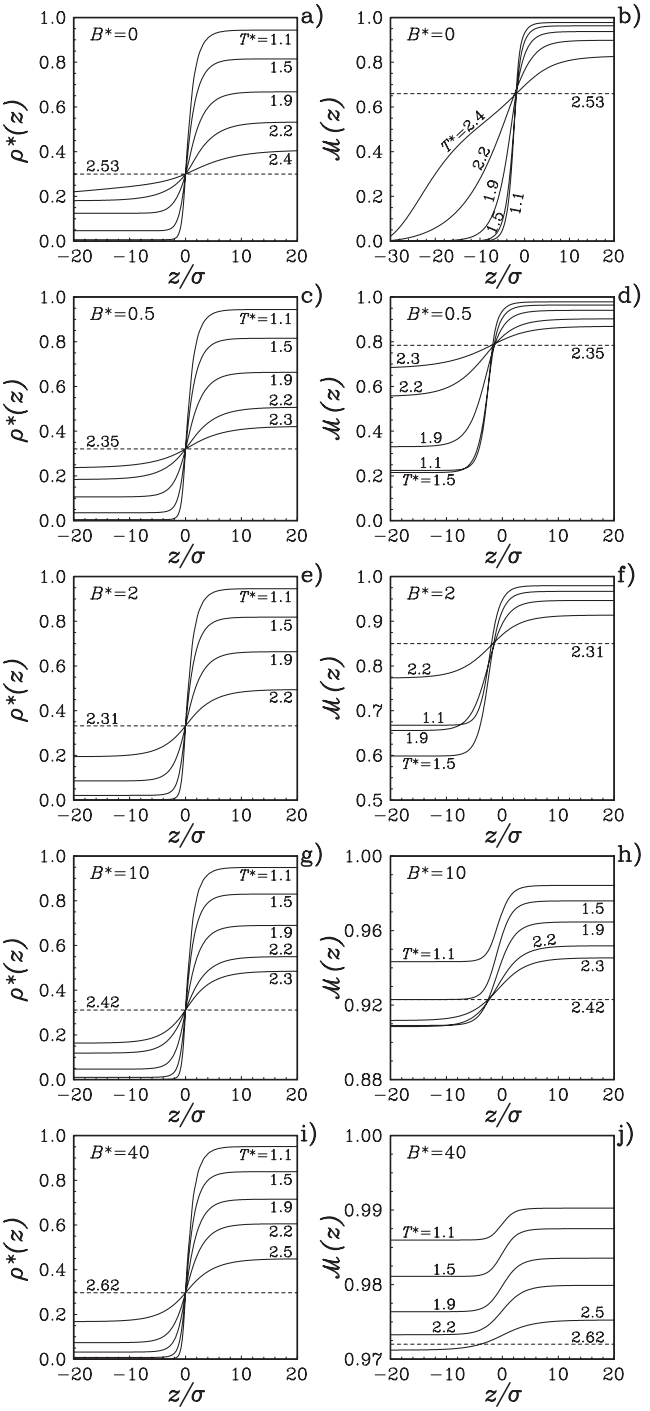

FIG. 1. The density $\rho^*(z)$ (left-hand subsets) and magnetization $\mathcal{M}(z)$ (right-hand subsets) profiles evaluated by the LMBW-AOZ-SMSA theory at the liquid-vapor interfaces of the XY fluid for different values of the external magnetic field, $B^*=0$, 0.5, 2, 10, and 40, as well as for various temperatures, $T^*=1.1$, 1.5, 1.9, and 2.2 up to subcritical values $T^*=2.3$, 2.4, or 2.5. The horizontal dashed lines correspond to critical temperatures.

Note that within the chosen system of coordinates, where $\rho(z=0,T,B)=\rho_c(B)$, the magnetization profiles $\mathcal{M}(z)$ related to different temperatures T do not intersect at $z=0$ for any given B. The reason is that at a fixed density the magnetization increases with decreasing temperature, as it can be seen

in Fig. 1 for the values of $\mathcal{M}(z=0)$ at different T and B. Surprisingly, for moderate external fields ($B^* \lesssim 2$), the intersection of the magnetization profiles $\mathcal{M}(z)$ occurs at some point $z_0 < 0$ shifted to the left-hand side. There $\mathcal{M}(z_0)$ is approximately equal to the magnetization $\mathcal{M}_c(B)$ at the critical temperature T_c [levels of critical density and magnetization are plotted in subsets (c)–(j) of Fig. 1 by horizontal dashed lines]. Such an unexpected behavior can be explained by the fact that the density becomes smaller along the interfaces when decreasing z. In turn this leads to decreasing the magnetization and, as a result, to the compensation of its rise due to lowering the temperature. For larger fields ($B^* \gtrsim 2$), the compensation fails and no one-point intersection can be observed.

In order to show that the number $\mathcal{N}=2$ of harmonics used is sufficient for the calculations we present the profiles of the expansion coefficients $a_0(z)$, $a_1(z)$, and $a_2(z)$ (see Figs. 2 and 3). One notices a monotonic decrease of $a_0(z)$ and a monotonic increase of $a_1(z)$ and $a_2(z)$ while switching shifting from the gas phase to the liquid phase. The values of $a_0(z)$ are always negative, whereas $a_1(z)$ and $a_2(z)$ are always positive. Such a dependence of the expansion coefficients follows from their definition [Eqs. (17) and (24)] and the behavior of the density [Eq. (22)] and magnetization [Eq. (23)] profiles (see Fig. 1). For the same reason, the families of functions $a_1(z)$ and $a_2(z)$, corresponding to different temperatures T and fixed external field B, intersect almost in the same point $z_0 \sim -2\sigma$ for any B, even in the saturation regime $B^* \gtrsim 40$. We see also in Figs. 2 and 3 that the magnitude of the expansion coefficients $a_n(z)$ rapidly decreases with increasing the number n of harmonics, i.e., $a_0 \gg a_1 \gg a_2$. For instance, the values of $a_2(z)$ are at least in two orders smaller compared to $a_1(z)$ even for large z when approaching the liquid phase. The ratio a_2/a_1 decreases further when shifting z to the gas side. A similar convergence was obtained for the harmonics coefficients c_{nml} and h_{nml} of the two-body correlation functions as well as for the virial pressure P. This insures that the number $\mathcal{N}=2$ of harmonics used is indeed enough for precise calculations and the influence of the higher-order terms can be neglected. The direct calculations have shown that the increase to $\mathcal{N}=3$ yields virtually unchanged results for all the investigated quantities.

The most interesting behavior can be observed for the density-orientation functions $\rho(z,\varphi)$. At each given value of B, these functions in the dimensionless form $\rho^*(z,\varphi) = \rho(z,\varphi)\sigma^3$ are plotted on the right-hand side of Fig. 3 for the characteristic temperature $T^*=1.9$ as a family of 10 curves corresponding to 10 different orientation angles varying from $\varphi=0$ to $\varphi=\pi$ in step of $\pi/9$. Remember that $\rho(z,\varphi)$ is an even function of φ, so that $\rho(z,-\varphi)=\rho(z,\varphi)$. Note that the orientation is defined with respect to the vector of the external magnetic field when $B \neq 0$ or with respect to the vector of the spontaneous magnetization for $B=0$. As it can be seen from the figure subsets, for any B the number of particles with parallel orientation of spins ($\varphi=0$) monotonically increases when going from the gas phase to the liquid state. For antiparallel spin orientation the pattern is completely inverse, i.e., the particle density monotonically decreases with increasing z. For intermediate orientations $0 < \varphi < \pi$, the

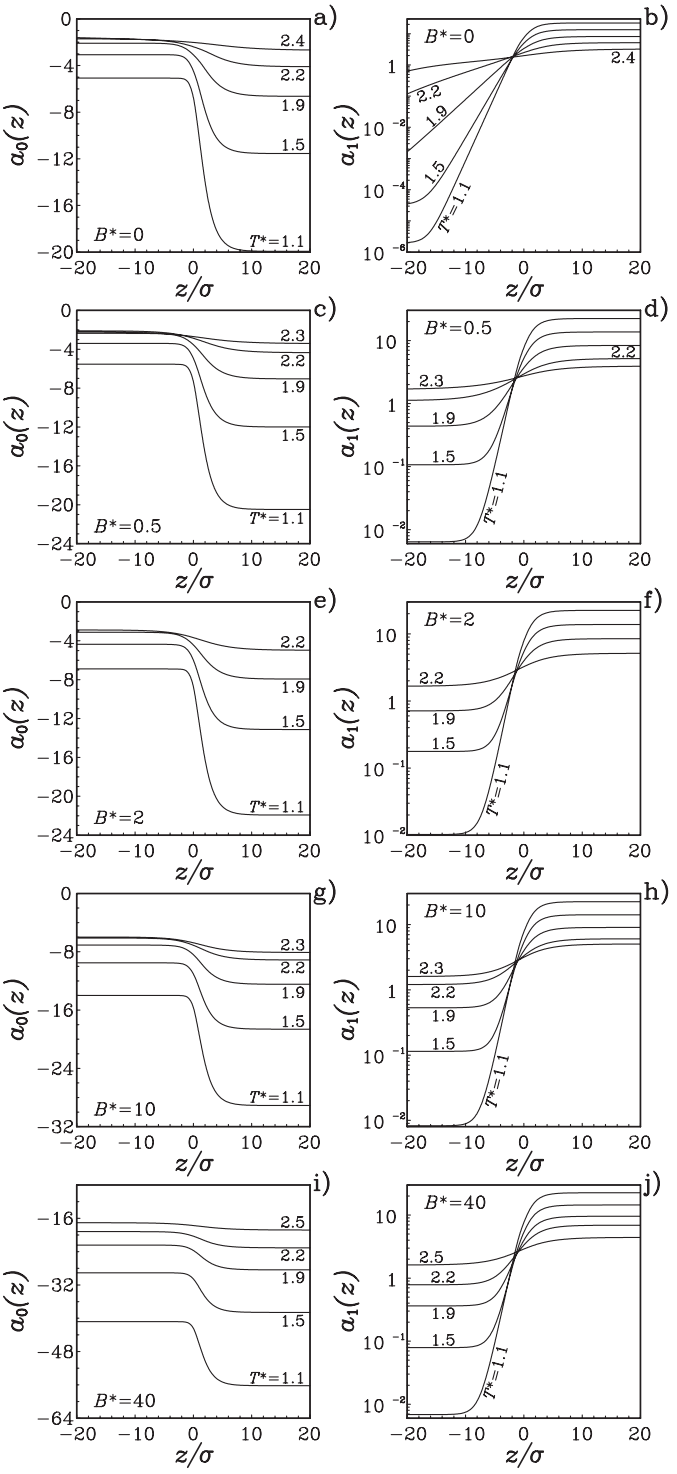

FIG. 2. The profiles for the zeroth- and first-order harmonics coefficients $a_0(z)$ and $a_1(z)$ of the one-body density-orientation function obtained within the LMBW-AOZ-SMSA approach at the liquid-vapor interfaces of the *XY* fluid for different values of the external magnetic field B and temperature T. Other notations are the same as for Fig. 1.

function $\rho(z,\varphi)$ can behave nonmonotonically in z with the existence of a maximum near the center $z=0$ of the profiles. Because of the nonmonotonicity, at each given B, there always exists some specific angle, $\varphi_s \sim \pi/3$, when the values

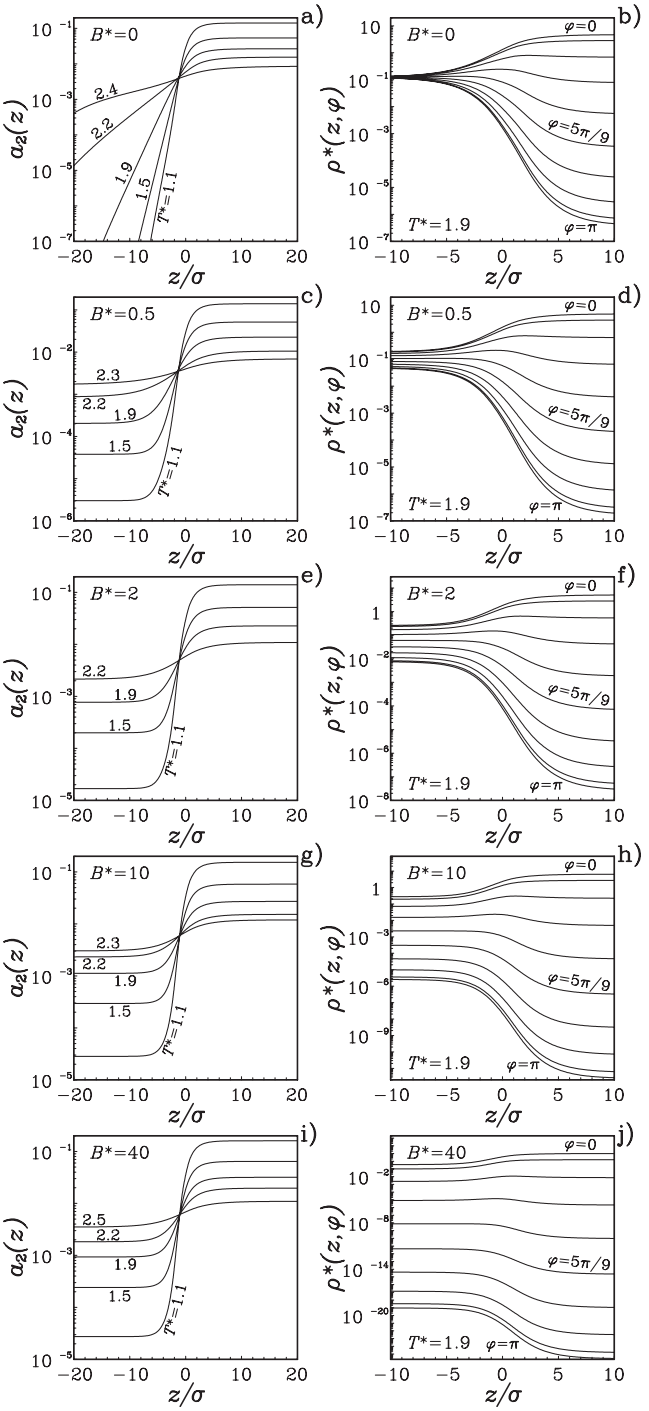

FIG. 3. The profiles for the second-order harmonics coefficient $a_2(z)$ and the density-orientation function $\rho(z,\varphi)$ predicted by the LMBW-AOZ-SMSA theory at the liquid-vapor interfaces of the *XY* fluid for various values of the external field B. The density function is plotted for various angles φ at the most characteristic fixed temperature of $T^*=1.9$. For other notations see Figs. 1 and 2.

for the one-body function in the gas and liquid phases are equal, i.e., $\rho(z\to-\infty,\varphi_s)=\rho(z\to\infty,\varphi_s)$.

Such a behavior of $\rho(z,\varphi)$ follows from the fact that in the case of ferromagnetic interactions [sign "−" at J in Eq. (1)] the parallel or nearly parallel $(\mathbf{s}_i\cdot\mathbf{s}_j>0)$ spin orientation is more preferable than the antiparallel $(\mathbf{s}_i\cdot\mathbf{s}_j<0)$ one. Therefore, the particles try to align parallel to each other and along the external magnetic field. In the paramagnetic gas state $(B=0,\ z\to-\infty)$ all the directions are equally probable, and the function $\rho(z,\varphi)$ does not depend on φ in this region of z [see subset (b) of Fig. 3]. Increasing the strength of the external field and shifting z in the direction of the liquid phase, the ratio of probabilities corresponding to parallel and antiparallel orientations increases. For weak external fields [$B^*\lesssim 2$, subsets (d) and (f) of Fig. 3], this increase is especially visible in the liquid state since then the magnetization rises rapidly with increasing density (see Fig. 1). When approaching the saturation regime [$B^*\gtrsim 10$, subsets (h) and (j) of Fig. 3], the external field will dominate over the internal one created by the interacting spins in the vapor phase because of the low gas density [$\rho_1^*\ll 1$, see subsets (g) and (i) of Fig. 1]. Then the density-orientation function can be approximately cast in the analytical form $\lim_{z\to-\infty}\rho(z,\varphi)\sim\exp(\beta B\cos\varphi)$. This leads to the ratio $\exp(2\beta B)$ of probabilities corresponding to parallel $(\cos\varphi=1)$ and antiparallel $(\cos\varphi=-1)$ orientations. It can be verified easily by direct comparison with the numerical results that this analytical representation can be used for quite good estimations. In particular, for $B^*=40$ one obtains from Fig. 3(j) that $\rho(z\to-\infty,\varphi=0)/\rho(z\to-\infty,\varphi=\pi)\approx 4\times 10^{19}$, while $\exp(2\beta B)=\exp(2\times 40/1.9)\approx 2\times 10^{19}$. The difference can be explained by the influence of the internal magnetic field. With going to the liquid phase, the influence increases further drastically giving a value $\rho(z\to\infty,\varphi=0)/\rho(z\to\infty,\varphi=\pi)\approx 4\times 10^{26}$.

In order to demonstrate a high consistency of the proposed LMBW-AOZ-SMSA theory, the asymptotic values $\lim_{z\to\mp\infty}\rho^*(z)$ and $\lim_{z\to\mp\infty}\mathcal{M}(z)$ of the liquid-vapor density and magnetization profiles are presented in Fig. 4 by circles in comparison with the corresponding bulk (solid curves) quantities $\rho_{1,2}^*$ and $\mathcal{M}_{1,2}=\mathcal{M}(a_1^{(1,2)},a_2^{(1,2)},\ldots,a_N^{(1,2)})$. We mention that the integration constants $a_1(0)$ and $a_2(0)$ and the parameter α of the interpolation of the direct correlation function were chosen in such a way as to provide the exact coincidence of the asymptotic and bulk values of the magnetization in the gas phase and the density in the liquid state, i.e., $\rho_2=\rho(\infty)$ and $\mathcal{M}_1=\mathcal{M}(-\infty)$. Then the asymptotic density $\lim_{z\to-\infty}\rho(z)$ in the vapor phase and the asymptotic magnetization $\lim_{z\to+\infty}\mathcal{M}(z)$ in the liquid phase will be the results of the integration of the LMBW equations. These results cannot be absolutely exact because of the approximations used for the direct correlation function which enters into the LMBW equations. Nevertheless, we readily see in Fig. 3 that the differences between ρ_1 and $\rho(-\infty)$ as well as between $\mathcal{M}_2$ and $\mathcal{M}(\infty)$ are quite small and almost invisible in the scale of the figures.

Note that contrary to $\rho_{1,2}$ and $\mathcal{M}_2$, the asymptotic gas magnetization $\mathcal{M}_1$ behaves nonmonotonically for $B\neq 0$ with changing temperature T. The nonmonotonicity follows from the fact that the magnetization $\mathcal{M}(\rho,T,B)$ is a function of three variables and it increases with increasing density ρ and decreasing temperature T. When moving down along the gas branch, both the density and temperature decrease. A decrease of density leads to a decrease of the magnetization if it takes place near the critical points. Here the effect of increas-

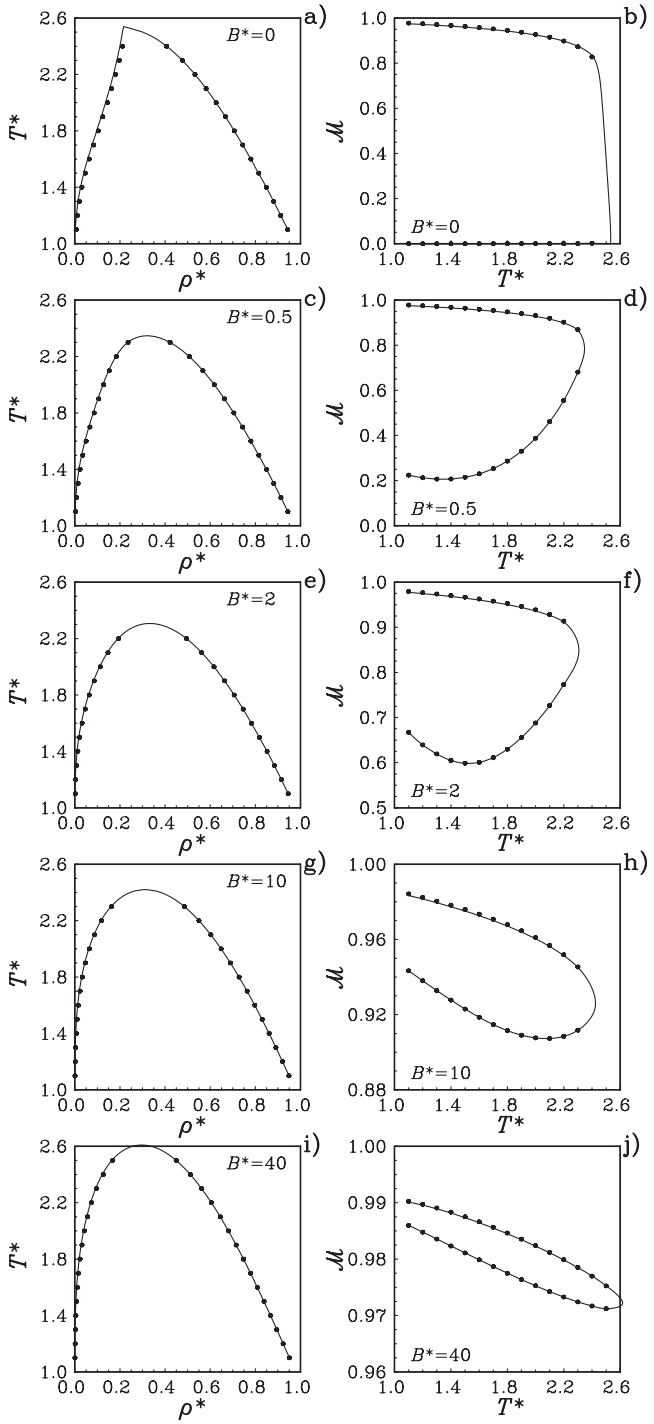

FIG. 4. The asymptotic densities $\rho(\pm\infty)$ (left-hand subsets) and magnetizations $\mathcal{M}(\pm\infty)$ (right-hand subsets) of the *XY* fluid at the liquid-vapor interfaces versus temperature, predicted by the inhomogeneous LMBW-AOZ-SMSA theory (circles) at different values of the external field in comparison with the corresponding bulk values $\rho_{1,2}$ and $\mathcal{M}_{1,2}$ obtained within the homogeneous description (solid curves).

ing the magnetization due to a slight decrease of T is negligible. However, at low enough temperatures, the gas density becomes very small (tends to zero) and practically does not change when moving along the binodal, while the temperature varies more rapidly. Then the effect of increasing the magnetization with decreasing the temperature begins to dominate resulting in the overall nonmonotonic behavior of $\mathcal{M}_1(\rho,T,B)$.

The asymptotic and bulk values of the second-order harmonics coefficient are plotted on the left-hand subsets of Fig. 5. In this case we also can observe a good agreement between the two sets of values. The deviations are insignificant and visible only on the liquid branch of the binodal at $B=0$ [subset (a)] or strong external fields $B^*\gtrsim 10$ [subsets (g) and (i)]. The influence of these deviations on the consistency of the results for the density and magnetization profiles is tiny since the magnitude of the second-order harmonics coefficient is several orders smaller than that of the lower-order ones.

The values for the parameter α (it enters into the interpolation coefficients for the direct correlation function) are shown in the right-hand subsets of Fig. 5 at different temperatures. A prominent feature of the dependence of this parameter on the temperature is that there exists a point, where α tends to zero (the level $\alpha=0$ is plotted by horizontal dashed curves). This happens in the interval $1.4\lesssim T^*\lesssim 1.65$ depending on the strength of B. The zeroth value of α means that no modification to the cubic interpolation used is necessary to obtain the self-consistency of the results. Here, the uncertainties coming from the approximate character of the SMSA closure and the interpolated direct correlation function are completely compensated by each other. On the other hand, the parameter α takes maximal values when approaching critical points. This is so because the SMSA closure does not work adequately in critical regions, and the modifications of the interpolation try to compensate the closure uncertainties. Note that these modifications concern only the metastable region and there their weight is equal to $\alpha/16$ (Sec. II D). We see that $\alpha\lesssim 5$ in the most range of B and T considered, where the weight $\alpha/16$ does not exceed a value of $5/16\sim 30\%$.

The density profiles $\rho^*(z)$ and their asymptotic values $\rho^*(\pm\infty)$ calculated by the inhomogeneous LMBW-AOZ-SMSA theory at the liquid-vapor interfaces of the *XY* fluid in the infinite external field limit $B\to\infty$ are shown for different temperatures as the solid curves and circles, respectively, in subsets (a) and (b) of Fig. 6. The bulk liquid-vapor coexisting densities $\rho^*_{1,2}$ corresponding to the homogeneous OZ-SMSA approach are plotted in subset (b) by the solid curve. Note that in the limit $B\to\infty$ the *XY* model can be reduced to a nonmagnetic isotropic Yukawa-like fluid with the interaction potential $\phi(r)=\varphi(r)-J(r)$. This is caused by the fact that at $B\to\infty$, all the spins align along the field vector **B**, i.e., $\cos\varphi_i=1$ and $\mathbf{s}_i\cdot\mathbf{s}_j=1$ for any i and j, so that $\lim_{B\to\infty}\mathcal{M}(z)\equiv 1$. The density profiles $\lim_{B\to\infty}\rho(z)$ behave similarly to the case of large values of B, where already $\mathcal{M}\approx 1$ because of the saturation [subsets (g)–(j) of Fig. 1]. As can be seen in subset (b) of Fig. 6, the deviations between the asymptotic and bulk densities are minimal, confirming an excellent self-consistency of the theory. The deviations will be larger (see the dashed curve) when the modification parameter α is chosen in such a way as to provide the coexistence of the asymptotic and bulk densities in the gas phase, instead of the liquid phase.

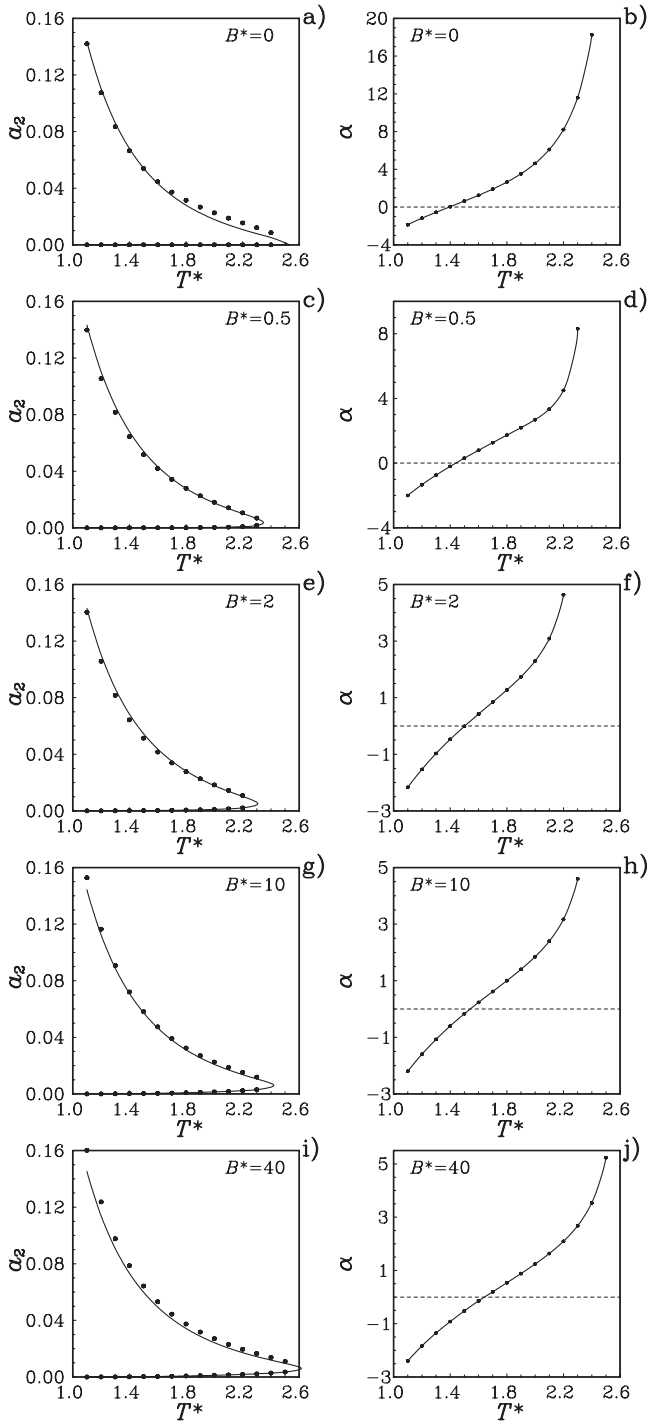

FIG. 5. The asymptotic values of the second harmonics coefficient $a_2(\pm\infty)$ (left-hand subsets) and the interpolation parameter α (right-hand subsets) as depending on temperature, obtained for the *XY* fluid at the liquid-vapor interfaces within the LMBW-AOZ-SMSA theory (circles) at different external fields. The bulk values of a_2 are plotted by solid curves.

No visible oscillations were found in the density $\rho(z)$ and magnetization $m(z)$ profiles in the range of T and B considered [see Figs. 1 and 6(a)]. This is in contrast to the case of nonmagnetic LJ-like systems, where a clear surface layering in the density has been established [8,35,36]. It was also

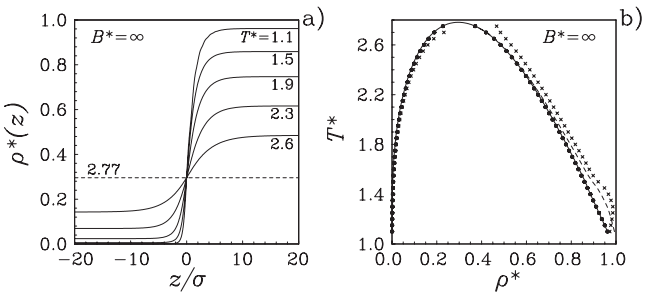

FIG. 6. The LMBW-AOZ-SMSA density profiles [solid curves, subset (a)] and their asymptotic values [circles and dashed curve, subset (b)] at the liquid-vapor interfaces of the *XY* fluid for $B=\infty$. The bulk gas and liquid densities are plotted in subset (b) by the solid curve. The asymptotic values obtained using an interpolation scheme of Refs. [8,35,36] are presented in subset (b) by the crosses.

shown [56,57] that simple liquids, with appropriate choices of the isotropic pair interaction, may exhibit oscillating behavior above the melting temperature. Notice, however, that the Yukawa function (used in the *XY* fluid to describe attractions between parallel spins) is much "softer" than potentials for typical liquid state models and thus exhibits less tendency towards layering packing [58,59]. Only at $T^*=1.1$ we identified the existence of very weak oscillationlike deviations from the monotonic increase of the *XY* density profiles when approaching the liquid phase. The amplitude of these deviations is quite small and invisible in the scale of Figs. 1 and 6(a). We can suppose that for lower temperatures ($T^*<1.1$) the oscillations will be stronger, but this requires a separate investigation which goes beyond the scope of this paper.

Note that the present approach is able to reasonably reproduce such subtle effects as the oscillating profile behavior despite the interpolation approximation used for the inhomogeneous direct correlation function. The reason is that this function behaves regularly in density even in the interfacial region (contrary to the total correlation function which can exhibit singularities there) [9,10]. We mention that the interpolation is performed with respect to density $\rho(z)$ and not with respect to coordinate z [see Eq. (27)], and the approximated two-body function depends on the distances z_1 and z_2 to the interface implicitly through the densities $\rho(z_1)$ and $\rho(z_2)$ taken at these distances [Eq. (25)]. For sufficiently low temperatures, the oscillating density profiles $\rho(z)$ can be obtained by solving the LMBW equations. Then the approximated function will also oscillate in coordinates z_1 and z_2 (like the exact inhomogeneous correlation function) because it (regularly) depends on $\rho(z_1)$ and $\rho(z_2)$.

For the purpose of comparison, we have also performed additional LMBW-AOZ-SMSA calculations using a somewhat other interpolation scheme. Namely, we considered the scheme by Iatsevitch and Forstmann (IF), which was intensively exploited in their works [8,35,36] on the investigation of LJ and LJ-like fluids. In the IF scheme, the coarse-grained density [Eq. (33)] is modified by shifting the interval of the integration as $\rho_{\sigma,\delta}(z)=\frac{1}{\sigma}\int_{z-\sigma/2+\delta}^{z+\sigma/2+\delta}\rho(z')dz'$. At the same time, no α-modifications [Eq. (30)] of the interpolation coefficients [Eq. (29)] are carried out. The shifting parameter δ takes over the role of the parameter α to achieve the consis-

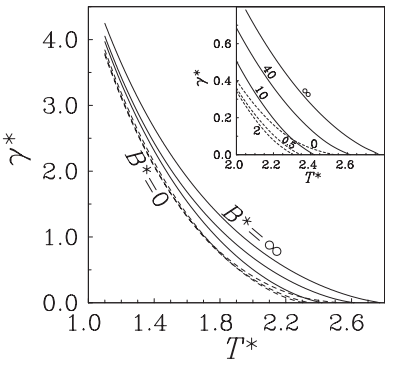

FIG. 7. The temperature dependence of the surface tension γ predicted by the LMBW-AOZ-SMSA theory for the *XY* fluid at different values of the external magnetic field, namely, $B^*=0$, 0.5, and 2 (dashed curves, top to bottom in the inset) as well as $B^*=10$, 40, and ∞ (solid curves, bottom to top). The inset is used to show the nonmonotonic behavior in detail.

tency of the results. The corresponding IF asymptotic values $\lim_{z\to\pm\infty}\rho^*(z)$ obtained at the liquid-vapor interfaces of the *XY* fluid in the limit $B\to\infty$ are added to subset (b) of Fig. 6 and shown by the crosses. In these calculations, the shifting parameter δ was adjusted (note that here $\alpha\equiv 0$) either to provide the exact coincidence of the asymptotic and bulk densities in the vapor or liquid phase. Then the asymptotic values of $\rho(z)$ in the liquid (right-hand side crosses) or in the vapor (left-hand side crosses) were the results of the LMBW integration. It can be seen clearly that in the case of δ interpolation the deviations (see the crosses) from the bulk values are much more significant with respect to those of our α-scheme (the circles and dashed curve).

Finally, the surface tension γ^* of the *XY* fluid is presented in Fig. 7 as a function of temperature T at fixed values of the external magnetic field, $B^*=0$, 0.5, 2, 10, 40, and ∞. This function monotonically decreases with increasing T at a given B. For $T\geqslant T_c(B)$ the surface tension is equal to zero, $\gamma(T,B)=0$, since the liquid-vapor interface does not exist in this case. It was shown in our previous investigations [44,45,47] by the mean field, integral equation, and simulation methods that the critical temperature $T_c(B)$ [and the critical density $\rho_c(B)$] of the *XY* fluid are nonmonotonic functions of B. Owing to this, the behavior of $\gamma(T,B)$ with varying B at a fixed T will be nonmonotonic as well. Indeed, as can be seen in the inset of Fig. 7, the surface tension first decreases with rising B from zero to $B^*=2$ and then increases reaching a maximum at infinite values of the external magnetic field.

IV. CONCLUSION

In summary, we have generalized the LMBW integro-differential equation approach to describe inhomogeneous properties of anisotropic magnetic fluids with *XY*-spin interactions. Our theory is based on the angle-harmonics expansion formalism for the interfacial one- and two-body correlation functions. The AOZ integral-equation scheme in conjunction with the SMSA closure were used for the calculation of bulk equilibrium quantities in the coexisting anisotropic phases. The self-consistency of the resulting LMBW-AOZ-SMSA theory has been provided by a proper interpolation of the two-particle direct correlation function in the interfacial region employing its bulk values. The inhomogeneous orientationally dependent one-particle density function has been obtained by solving the LMBW equations. As a result, the density and magnetization profiles at the planar liquid-vapor interfaces of the *XY* fluid as well as the surface tension have been calculated in the absence and presence of an external magnetic field for a wide range of temperatures including subcritical regions. The proposed LMBW-AOZ-SMSA theory can be extended to more complicated models of magnetic fluids with anisotropic spin interactions as well as to magnetic fluid mixtures.

ACKNOWLEDGMENTS

This work was supported in part by the Fonds zur Förderung der Wissenschaftlichen Forschung under Contract No. 18592-PHY. A.K. acknowledges the support from the National Research Council (NRC) of Canada.

[1] *Fundamentals of Inhomogeneous Fluids*, edited by D. Henderson (Dekker, New York, 1992), Vol. 10.
[2] *Liquid Interfaces in Chemical, Biological and Pharmaceutical Applications*, Surfactant Science Series, edited by A. G. Volkov (Marcel Dekker, New York, 2001), Vol. 95.
[3] J. P. Hansen and I. R. McDonald, *Theory of Simple Liquids*, 2nd ed. (Academic, London, 1986).
[4] C. Caccamo, Phys. Rep. **274**, 1 (1996).
[5] R. Lovett, C. Y. Mou, and F. P. Buff, J. Chem. Phys. **65**, 570 (1976).
[6] M. S. Wertheim, J. Chem. Phys. **65**, 2377 (1976).
[7] J. Fischer and M. Methfessel, Phys. Rev. A **22**, 2836 (1980).
[8] S. Iatsevitch and F. Forstmann, J. Chem. Phys. **107**, 6925 (1997).
[9] I. Omelyan, A. Kovalenko, and F. Hirata, Chem. Phys. Lett. **397**, 368 (2004).
[10] I. Omelyan, F. Hirata, and A. Kovalenko, Phys. Chem. Chem. Phys. **7**, 4132 (2005).
[11] S. Toxvaerd, J. Chem. Phys. **64**, 2863 (1976).
[12] A. M. Somoza, E. Chacoón, L. Mederos, and P. Tarazona, J. Phys.: Condens. Matter **7**, 5753 (1995).
[13] H. T. Davis, *Statistical Mechanics of Phases, Interfaces, and Thin Films* (VCH, New York, 1996).
[14] I. Napari, A. Laaksonen, V. Talanquer, and D. W. Oxtoby, J. Chem. Phys. **110**, 5906 (1999).
[15] V. Talanquer and D. W. Oxtoby, J. Chem. Phys. **103**, 3686 (1995); **113**, 7013 (2000).
[16] J. Winkelmann, J. Phys.: Condens. Matter **13**, 4739 (2001).

[17] P. S. Christopher and D. W. Oxtoby, J. Chem. Phys. **117**, 9502 (2002).
[18] P. Geysermans, N. Elyeznasni, and V. Russier, J. Chem. Phys. **123**, 204711 (2005).
[19] F. P. Buff, R. A. Lovett, and F. H. Stillinger, Jr., Phys. Rev. Lett. **15**, 621 (1965).
[20] J. D. Weeks, J. Chem. Phys. **67**, 3106 (1977).
[21] M. Robert, Phys. Rev. Lett. **54**, 444 (1985).
[22] J. Stecki, J. Chem. Phys. **107**, 7967 (1997).
[23] D. J. Lee, M. M. Telo da Gama, and K. E. Gubbins, Mol. Phys. **53**, 1113 (1984).
[24] C. D. Holcomb, P. Clancy, and J. A. Zollweg, Mol. Phys. **78**, 437 (1993).
[25] J. Stecki and S. Toxvaerd, J. Chem. Phys. **105**, 4191 (1996).
[26] M. Mecke, J. Winkelmann, and J. Fischer, J. Chem. Phys. **107**, 9264 (1997).
[27] I. Benjamin, Annu. Rev. Phys. Chem. **48**, 407 (1997).
[28] J. J. Potoff and A. Z. Panagiotopoulos, J. Chem. Phys. **112**, 6411 (2000).
[29] D. O. Dunikov, S. P. Malyshenko, and V. V. Zhakhovskii, J. Chem. Phys. **115**, 6623 (2001).
[30] J. R. Errington, Phys. Rev. E **67**, 012102 (2003).
[31] V. Simmons and J. B. Hubbard, J. Chem. Phys. **120**, 2893 (2004).
[32] E. Diaz-Herrera, J. A. Moreno-Razo, and G. Ramirez-Santiago, Phys. Rev. E **70**, 051601 (2004).
[33] S. M. Thompson and K. E. Gubbins, J. Chem. Phys. **70**, 4947 (1979).
[34] J. Eggebrecht, K. E. Gubbins, and S. M. Thompson, J. Chem. Phys. **86**, 2286 (1987).
[35] S. Iatsevitch and F. Forstmann, Mol. Phys. **98**, 1309 (2000).
[36] S. Iatsevitch and F. Forstmann, J. Phys.: Condens. Matter **13**, 4769 (2001).
[37] P. I. C. Teixeira and M. M. Telo da Gama, J. Phys.: Condens. Matter **14**, 12159 (2002).
[38] F. Bresme and J. Faraudo, J. Phys.: Condens. Matter **19**, 375110 (2007).
[39] A. Kovalenko and F. Hirata, Phys. Chem. Chem. Phys. **7**, 1785 (2005).
[40] I. P. Omelyan, R. Folk, I. M. Mryglod, and W. Fenz, J. Chem. Phys. **126**, 124702 (2007).
[41] K. Moon and S. M. Girvin, Phys. Rev. Lett. **75**, 1328 (1995).
[42] D. J. Tulimieri, J. Yoon, and M. H. W. Chan, Phys. Rev. Lett. **82**, 121 (1999).
[43] A. Maciołek, M. Krech, and S. Dietrich, Phys. Rev. E **69**, 036117 (2004).
[44] I. P. Omelyan, W. Fenz, I. M. Mryglod, and R. Folk, Phys. Rev. Lett. **94**, 045701 (2005).
[45] I. P. Omelyan, W. Fenz, I. M. Mryglod, and R. Folk, Phys. Rev. E **72**, 031506 (2005).
[46] F. Lado and E. Lomba, Phys. Rev. E **76**, 041502 (2007).
[47] W. Fenz, R. Folk, I. M. Mryglod, and I. P. Omelyan, Phys. Rev. E **68**, 061510 (2003).
[48] I. P. Omelyan, I. M. Mryglod, R. Folk, and W. Fenz, Phys. Rev. E **69**, 061506 (2004); **70**, 049903(E) (2004).
[49] W. Fenz, I. P. Omelyan, and R. Folk, Phys. Rev. E **72**, 056121 (2005).
[50] I. P. Omelyan, W. Fenz, R. Folk, and I. M. Mryglod, Eur. Phys. J. B **51**, 101 (2006).
[51] W. G. Madden and S. A. Rice, J. Chem. Phys. **72**, 4208 (1980).
[52] N. Choudhury and S. K. Ghosh, J. Chem. Phys. **116**, 8517 (2002).
[53] D. G. Triezenberg and R. Zwanzig, Phys. Rev. Lett. **28**, 1183 (1972).
[54] A. Kovalenko, S. Ten-no, and F. Hirata, J. Comput. Chem. **20**, 928 (1999).
[55] I. P. Omelyan and V. B. Solovyan, J. Comput. Appl. Math. **188**, 190 (2006).
[56] E. Chacón, M. Reinaldo-Falagán, E. Velasco, and P. Tarazona, Phys. Rev. Lett. **87**, 166101 (2001).
[57] E. Velasco, P. Tarazona, M. Reinaldo-Falagán, and E. Chacón, J. Chem. Phys. **117**, 10777 (2002).
[58] A. J. Archer, P. Hopkins, and R. Evans, Phys. Rev. E **74**, 010402(R) (2006).
[59] P. Hopkins, A. J. Archer, and R. Evans, J. Chem. Phys. **124**, 054503 (2006).